Red Blood Cells Augment Leukocyte Rolling in a Virtual Blood Vessel

Cristiano Migliorini,* YueHong Qian,† Hudong Chen,† Edward B. Brown,* Rakesh K. Jain,* and Lance L. Munn*

*Departments of Radiation Oncology, Massachusetts General Hospital and Harvard Medical School, Boston, Massachusetts 02114 USA; and †Exa Corporation, Lexington, Massachusetts 02420 USA

ABSTRACT Leukocyte rolling and arrest on the vascular endothelium is a central event in normal and pathological immune responses. However, rigorous estimation of the fluid and surface forces involved in leukocyte-endothelial interactions has been difficult due to the particulate, non-Newtonian nature of blood. Here we present a Lattice-Boltzmann approach to quantify forces exerted on rolling leukocytes by red blood cells in a "virtual blood vessel." We report that the normal force imparted by erythrocytes is sufficient to increase leukocyte binding and that increases in tangential force and torque can promote rolling of previously adherent leukocytes. By simulating changes in hematocrit we show that a close "envelopment" of the leukocyte by the red blood cells is necessary to produce significant changes in the forces. This novel approach can be applied to a large number of biological and industrial problems involving the complex flow of particulate suspensions.

INTRODUCTION

Red blood cells (RBCs) constitute ~40% of the volume of blood. They are deformable biconcave disks that preferentially flow in the center of vessels, rather than near the wall, leaving a plasma-rich zone of 2 to 6 μm near the endothelial layer (Phibbs, 1968; Blackshear et al., 1971; Skalak and Chien, 1987). There are far fewer circulating leukocytes, or white blood cells (~1000 RBCs for every leukocyte), the cells that police the vasculature searching for areas of inflammation or pathology. A comprehensive biophysical description of this process would allow development of novel treatment strategies for many diseases, including atherosclerosis, arthritis, and cancer. But to date, this goal has been elusive due to the complexities of the fluid dynamics and cell-surface interactions involved.

The process of leukocyte adhesion in vivo consists of dynamic adhesion (rolling on endothelial wall) followed by stable adhesion and extravasation into the target organ. Rolling is mediated by transient interactions between adhesion molecules on the leukocyte surface and their receptors on the endothelium. These adhesion molecules are located on microvilli, small protuberances of 300 to 700 nm on the cell surface, whereas their counterparts on the endothelial wall lay within the glycocalyx layer, which extends 50 to 500 nm above the endothelial plasma membrane (Zao et al., 2001).

In vitro studies of leukocyte rolling are generally carried out using dilute cell suspensions in flow chambers, which provide a controlled, defined geometry (usually between parallel plates) as the flowing cells interact with ligands or cell monolayers at the surface (Munn et al., 1996). These experiments have been useful for translating the molecular binding properties of individual adhesion molecules into dynamic force analyses using mathematical models (Zao et al., 2001; Chang and Hammer, 1996). Unfortunately, to isolate the biomolecular mechanisms of cell-surface ligand-receptor interactions, flow chamber experiments and mathematical simulations have traditionally used RBC-free systems (i.e., saline suspensions) in which the complexities of blood rheology are not reproduced.

In previous experimental work, red blood cells have shown a remarkable capacity to enhance (Munn et al., 1996; Melder et al., 1995) leukocyte-endothelial wall interactions or to affect leukocyte-leukocyte (Mitchell et al., 2000) interactions both in vitro and in vivo (Melder et al., 2000). These results and previous investigations on the flow dynamics of deformable particulate suspensions (Schmid-Schönbein et al., 1975) clearly show that the cell adhesion process in vivo is strongly affected by RBCs.

In this work we present the first mathematical model for leukocyte rolling and adhesion in which the effect of the RBCs is explicitly addressed. This model mimics the in vivo flow dynamics by simulating suspensions of rigid particles using a Lattice Boltzmann technique. In the two-dimensional simulations presented here, leukocytes are modeled as discs rolling on and interacting with a flat wall through transient ligand-receptor binding, whereas RBCs are modeled as ellipses (Fig. 1).

Our Lattice Boltzmann model constitutes a significant improvement over previous methods by providing the full solution of the fluid dynamics of the particle suspension in a confined geometry. The flow dynamics are coupled with a stochastic model of receptor-ligand binding to produce a detailed description of leukocyte-endothelial wall interaction. This approach allows us to reproduce the dynamics of leukocyte adhesion in postcapillary venules, where the vessel diameter is approximately twice that of the cell. In

Submitted December 19, 2001, and accepted for publication May 24, 2002.

Address reprint requests to: Lance L. Munn, Department of Radiation Oncology, Massachusetts General Hospital, 3409 Building 149, Charlestown, MA 02129; Tel.: 617-726-4085; Fax: 617-726-1962; E-mail: lance@steele.mgh.harvard.edu.

For additional information and simulation movies, see http://steele.mgh.harvard.edu.

0006-3495/02/10/1834/08 $2.00

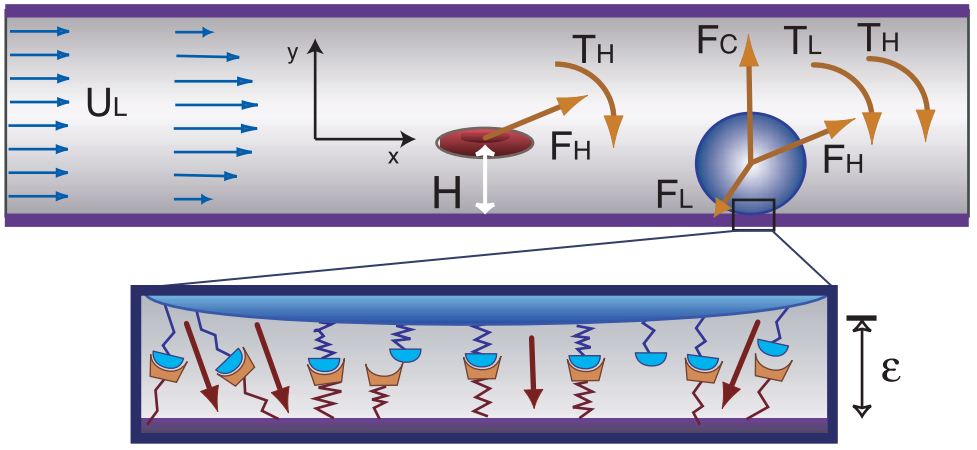

FIGURE 1 Disk representing a leukocyte is rolling on the wall of a capillary. The leukocyte interacts with the wall through receptor-ligand interactions and an empirical repulsive van der Waals force. The forces and torques of individual bonds are summed (F_L, T_L) and applied to the leukocyte together with the colloidal (F_c) and hydrodynamic force and the torque (F_H, T_H). The ellipse mimicking an RBC is introduced at left with its major axis parallel to the wall. Three cases are considered: case A, where only the leukocyte is present; case B, where an RBC is introduced at a distance of 2 tube diameters from the leukocyte with initial height H equal to the radius of the leukocyte. Case C is identical to case B, except that the initial height H is one-half the tube diameter. Parameter definitions are summarized in Table 1.

addition, our model allows characterization of the collision between RBCs and rolling leukocytes. Thus, our model provides the first quantification of forces imparted by RBCs on rolling leukocytes and allows detailed analysis of the mechanisms of interaction. As an example of model application, we show how changes in blood hematocrit (i.e., RBC concentration) affect the forces of interaction.

MATERIALS AND METHODS

Multiphoton microscopy of blood flow

It has been hypothesized that one mechanism for enhanced leukocyte-endothelial wall interactions in the presence of RBCs may be the enrichment of leukocyte concentration near the vessel wall (Munn et al., 1996; Melder et al., 1995). To investigate this possibility, we measured the concentration profiles of leukocytes flowing in the parallel plate flow chamber with and without RBCs using multiphoton microscopy (Brown et al., 2001). The 780-nm laser scanned through the entire height of the flow chamber (75 μm), allowing measurement of the leukocyte flux at 14 positions between the parallel plates. The use of a 30 X/0.9 NA long working distance objective lens limited the vertical resolution to 5 microns. A suspension of 2×10^6 leukocyte/mL (DAUDI) labeled with hexidium iodide (520/600 nm, Molecular Probes, Eugene, OR) in 30% hematocrit RBCs was used in the experiments. The suspending medium was either saline or a dextran solution (3% by weight, 300 kDa) (Cokelet and Goldsmith, 1991). In the relevant range of shear rates (Munn et al., 1996; Melder et al., 1995), no significant deviations in the leukocyte concentrations were seen near the wall of the flow chamber (data not shown), indicating that concentration enhancement does not contribute to RBC enhancement of leukocyte-endothelial wall interactions.

Leukocyte-wall interactions

The model used in this work is based on previous models used by several groups (Zao et al., 2001; Chang and Hammer, 1996; Hammer and Apte, 1992; Dong et al., 1999). Adhesion molecules are modeled as adhesive springs, distributed uniformly over the leukocyte surface. The leukocyte is initially placed in proximity of the wall so that bond formation is possible. The wall is assumed to contain a high density of receptor molecules and is uniformly reactive (Chang and Hammer, 1996).

The procedure for the simulation follows two steps. At time t, the state of bound and unbound molecules is updated by Monte Carlo lottery. It is assumed that the rate of bond formation k_f is equal to its maximal value (Chang et al., 2000). Therefore, if the height of a ligand y_l is less than a critical value H_c, bond formation may happen with a finite probability P_f, according to (for symbols, see Table 1) (Chang et al., 2000; Dong et al., 1999):

$$P_f = 1 - \exp(-k_{on}\Delta t) \quad y_l \le H_c \tag{1}$$

in which $k_{on} = k_f \times N_L$. A preexisting bond may be broken with probability P_r, which increases with its current load:

$$P_r = 1 - \exp(-k_r\Delta t) \quad k_r = k_r^0 \exp\left(\frac{(\sigma - \sigma^*)(L - \lambda)^2}{2k_bT}\right) \tag{2}$$

The force applied by the bond on the rolling leukocyte along the receptor-ligand direction is given by:

$$f = \sigma(L - \lambda) \tag{3}$$

The forces contributed by the individual ligand-receptor bonds are summed to determine the total bond forces and the torque acting on the cell during the period Δt. The parameters for the simulations are given in Table 1. In our simulations, $\sigma > \sigma^*$.

Nonspecific repulsive forces between the leukocyte and the wall are accounted for using an empirical van der Waals potential interaction using a Derjaguin approximation. The force per unit length (Israelachvili, 1985; Bongrand and Bell, 1984) is:

$$F_C = \frac{A}{8\sqrt{2}}\sqrt{\frac{R_C}{\varepsilon^5}} \tag{4}$$

in which ϵ is the separation between the surfaces. Although other empirical expressions can be used to prevent contact between the leukocyte and the

TABLE 1 Symbols

Parameter	Definition	Value (ref.)
	Major axis Ellipse	4.2 μm (Skalak and Chien, 1987)
	Minor axis Ellipse	1.2 μm (Skalak and Chien, 1987)
	Wall shear rate	142 s^{-1} (Munn et al., 1996)
	Wall shear stress	0.17 Pa
A	Repulsive Hamaker constant	5 10^{-20} J (Bongrand and Bell, 1984; Israelachvili, 1985)
D	Tube diameter	20 10^{-6} m (Skalak and Chien, 1987)
F_c	Repulsive force per unit length	–
H_C	Critical height	40 10^{-9} m (Chang et al., 2000)
k_b	Boltzmann constant	
k_f	Forward reaction rate	85 s^{-1} (Chang et al., 2000)
k_r	Reverse reaction rate	
k_r^0	Intrinsic reverse reaction rate	1 10^{-2} s^{-1} (Chang and Hammer, 1996)
L	Bond length	–
N_L	Ligand density*	47/μm^2 (Chang and Hammer, 1996)
P_f	Probability of bond formation	
P_r	Probability of bond breakage	
R_c	Disk radius	4.5 μm (Skalak and Chien, 1987)
Re	Reynolds number (L D/ν)	8.07 10^{-3} (Chapman and Cokelet, 1997)
T	Temperature	310 K (Chang and Hammer, 1996)
u_L	Inlet velocity	4.8 10^{-4} m/s
y_l	Bond length	
ε	Separation distance	
λ	Equilibrium bond length	20 nm (Chang and Hammer, 1996)
ν	Plasma kinematic viscosity	1.2 10^{-6} m^2/s (Skalak and Chien, 1987)
ρ_c	Disk density	1070 Kg/m^3 (Skalak and Chien, 1987)
ρ_d	Ellipse density	1098 Kg/m^3 (Skalak and Chien, 1987)
ρ_f	Fluid density	1000 Kg/m^3 (Skalak and Chien, 1987)
σ	Spring constant	2 10^{-3} N/m (Chang and Hammer, 1996)
σ^*	Transition state spring constant	1 10^{-3} N/m (Chang and Hammer, 1996)

*600 ligands distributed around the cylinder circumference spaced every 0.45 μm.

wall and the corresponding mathematical singularity (King and Hammer, 2001), the use of an empirical van der Waals potential is justified because it exhibits the same behavior as the rigorous repulsive expressions that include steric and electrostatic forces (Bongrand and Bell, 1984). F_c is applied to the center of the leukocyte and is normal to the wall.

Flow dynamic model

A Lattice Boltzmann method for the analysis of fluid suspensions is used to calculate the unsteady flow field and the particle dynamics. This technique is an improvement over the original algorithm proposed by Ladd (1994) and is a robust method for simulating the dynamics of impermeable particle suspensions with inertia and any solid-to-fluid density ratio (Aidun et al., 1998). Although the lattice Boltzmann approach can effectively be adapted to three-dimensional systems, our current work is limited to the two-dimensional case. However, it is worth noting that in small gaps between capillaries and cells the stress field has a two-dimensional behavior, and therefore two-dimensional model predictions are accurate for the geometry we have chosen (Graver and Kute, 1998). The method is based on the solution of the Lattice Boltzmann equations on a square lattice with nine directions for the fluid phase (2DQ9) (Qian et al., 1992). This is coupled through solid-fluid interaction rules to the Newtonian rotation and translation of solid particles suspended in the fluid (Aidun et al., 1998). It is well established that with an appropriate equilibrium distribution function and suitable physical limits, the Lattice Boltzmann will reduce to the full Navier-Stokes equations (Qian et al., 1992; Chen et al., 1992).

Two sets of solid particles are considered in this work: disks and ellipses of infinite depth, representing leukocytes and RBCs, respectively (Fig. 1). In our simulations, the rolling leukocyte is influenced not only by hydrodynamic forces but also by the repulsive force from the wall and by the stochastic interactions of receptors distributed on the leukocyte with ligands on the wall as described in the previous section (Fig. 1). The RBCs are only affected by hydrodynamic forces.

The simulations of three cases (A, B, and C) were designed to allow full development of flow profiles and to avoid boundary effects. The inlet boundary condition was a uniform velocity profile u_L, and a stress-free condition was applied at the tube outlet (Aidun et al., 1998). Calculations were carried out using a 1200 $\times$ 67 lattice grid, which is sufficient to provide numerical convergence (Aidun et al., 1998; Bernsdorf et al., 1998). The Lattice Boltzmann relaxation time τ was 1, corresponding to a time step of 1.25 $\times$ 10^{-8} s. The forces and torques reported in this work were calculated for a cell of 9-μm diameter (Table 1) and were averaged over 50 μs using a moving average algorithm.

RESULTS

Case A: leukocyte rolling in the absence of RBCs

In case A, the leukocyte rolls in response to the flowing Newtonian fluid, dynamically forming and breaking bonds with the surface (see movies of the simulations in the Supplementary Material). The results of case A compare very well with data in the literature. The average value of 60 pN (Fig. 2) calculated for the tangential force (x direction in Fig. 1) is in very good agreement with results from numerical simulations (Dong et al., 1999; Graver and Kute, 1998)

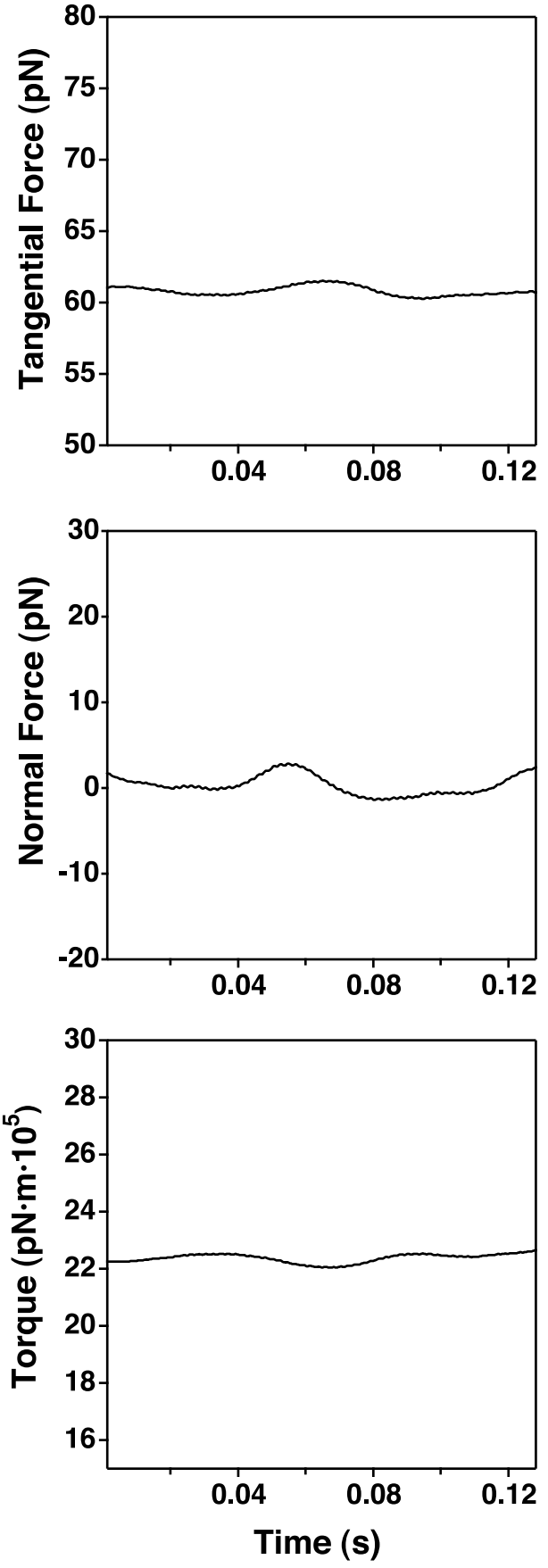

and the analytical solution of Goldman et al. (1967). These results are also consistent with model studies by Schmidt-Schönbein et al. (1980) and Chapman and Cokelet (1997) and theoretical predictions by Fung (1984) (Table 2). The same is true for the calculation of the torque, which is 23×10^{-5} pN m^{-1} (Fig. 2) and for the pressure drop across the disturbed region of flow, which is 1.2 Pa (Graver and Kute, 1998; Chapman and Cokelet, 1997).

There is a paucity of values for normal forces (y direction in Fig. 1) available in the literature. Our model predicts an average value of 0.27 pN away from the surface (Fig. 2). Experimental results on the repulsion of RBCs from tube walls have provided values varying from 0.36 to 1.8 pN (Blackshear et al., 1971), depending on shear rate and cell deformability. Although the absolute value of this force is small compared with the tangential force, the repulsive force plays a crucial role in the process of leukocyte rolling. In fact, in a simulation without receptor-ligand interactions and colloidal forces, this small positive repulsive force is able to drive the cell away from the tube wall.

One commonly measured experimental parameter is rolling velocity. The average rolling velocity for case A was 186 μm/s. This compares favorably with experimental results under similar conditions (Munn et al., 1996).

Case B: collision between RBC and rolling leukocyte

The hydrodynamic interaction transmitted by the small fluid lubrication layer between the passing RBC and the leukocyte (Fig. 3 *A*) is responsible for a significant increase in the average tangential force and torque (~10%) during collision, accompanied by an increase in rolling velocity (10%). Dramatic changes are also seen in the normal force (Fig. 3 *B*, Table 2). Note that the peak forces can be much larger than the average values.

At the onset of collision, the RBC causes the normal hydrodynamic force to change sign (net downward force) and the torque and tangential force on the leukocyte to increase (Fig. 3). As the RBC slips past the leukocyte (Fig. 3 *A*), the normal force again becomes positive. At this point the torque and tangential force go through another peak. The simulation results show that the modulation of the normal force is due to a pressure changes on the order of 0.5 Pa between the RBC and the leukocyte.

The main results of case B are as follows: 1) the RBC trajectory is strongly affected in case B, flipping 180° after the collision (see Fig. 3 *A*). The velocity of the RBC before collision is 500 μm/s; during collision it decelerates to 300 μm/s and then accelerates to 700 μm/s as it is forced into

FIGURE 2 Case A simulates simple rolling of a leukocyte on a receptor-coated surface in response to fluid flow. Hydrodynamic tangential force, normal force, and torque profiles are shown.

TABLE 2 Study results

	Normal force pN	Tangential force PN	Torque pN × m × 10^5	Pressure drop Pa	Rolling velocity μm/s
Literature Data	0.36–1.8 (Blackshear et al., 1991)	45–450 (Dong et al., 1999; Graver and Kute, 1998; Goldman et al., 1967; Chapman and Cokelet, 1997)	14–81 (Graver and Kute, 1998; Goldman et al., 1967)	1.3–4.5 (Graver and Kute, 1998; Chapman and Cokelet, 1997)	25–225 (Munn et al., 1996)
Case A	0.27	60	23	1.2	186
Case B	0.18 (−33%)	67 (+11%)	25.2 (+11%)	–	197 (+6%)
Case C	0.22 (−18%)	63 (+5%)	23.4 (+1.5%)	–	190 (+2%)

the higher velocity fluid (Fig. 4). 2) Compared with the free-rolling disk, the magnitudes of the hydrodynamic forces and torques are significantly different. Clear increases in tangential force and torque (evidenced by two peaks) result. The average extent of this interaction is ~10% over the baseline value. 3) The magnitude and direction of the normal force changes significantly. After head-on collision the normal force becomes large and negative (favoring adhesion). It is interesting that the normal force required by a microvillus to penetrate the glycocalyx is on the order of 2.8 to 14 pN (Zao et al., 2001), which is very close to the negative hydrodynamic force provided by the RBC in the case B head on collision (−15 pN). This force is applied for 10 to 20 ms, a sufficient time to allow glycocalyx penetration (Zao et al., 2001).

These results are not very sensitive to the wall shear rate. With the same parameters, except at a shear rate of 71 s^{-1}, we get smaller values for the baseline tangential force (35 pN), torque (9 pN), and rolling velocity (87 μm/s). However, the increase in rolling velocity, torque, and tangential

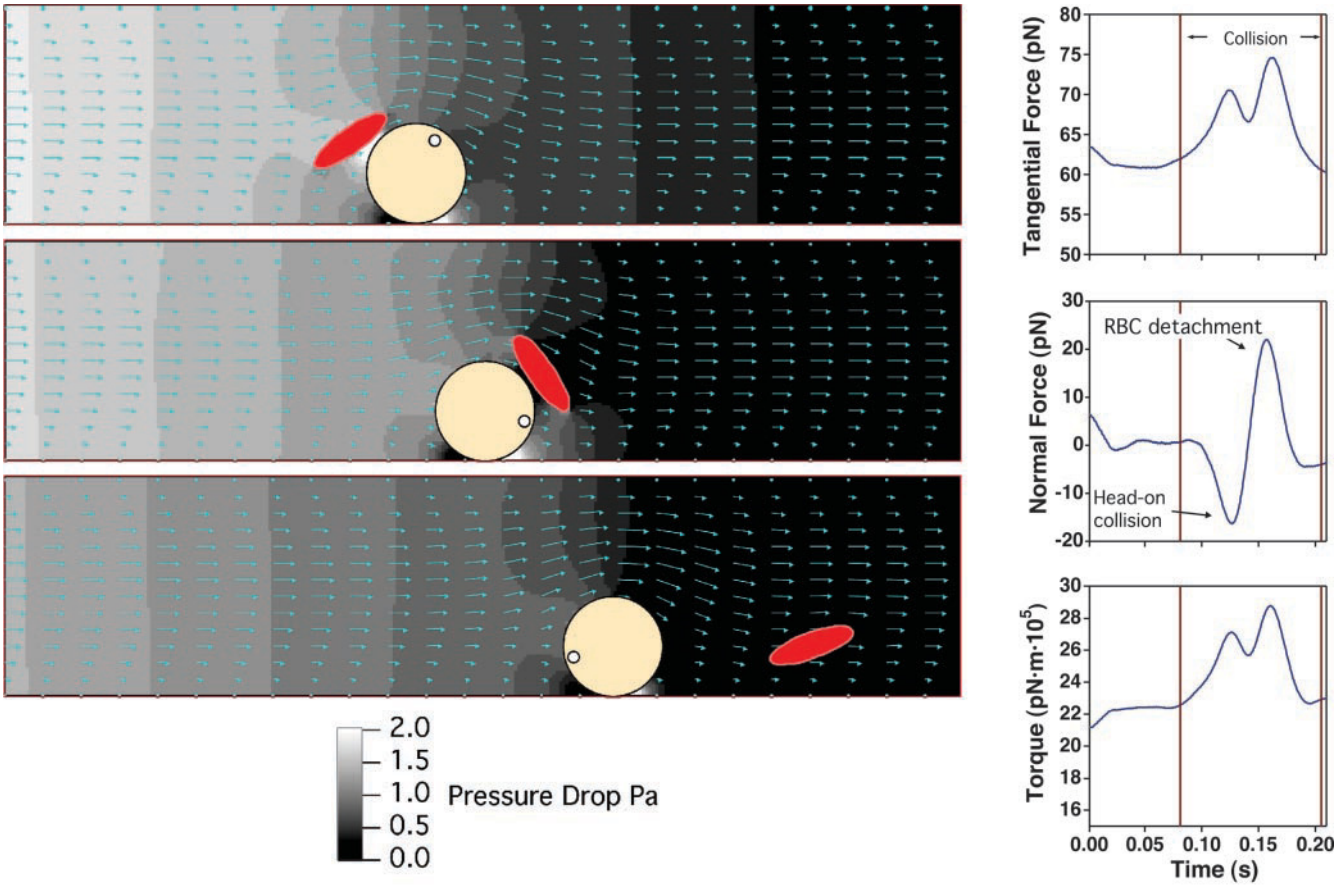

FIGURE 3 Case B simulates a collision between a passing RBC and the rolling leukocyte at the midpoint of the leukocyte. (*left*) Flow field at time t = 0.125, 0.157, 0.219 s. (*right*) Hydrodynamic tangential force, normal force, and torque profile.

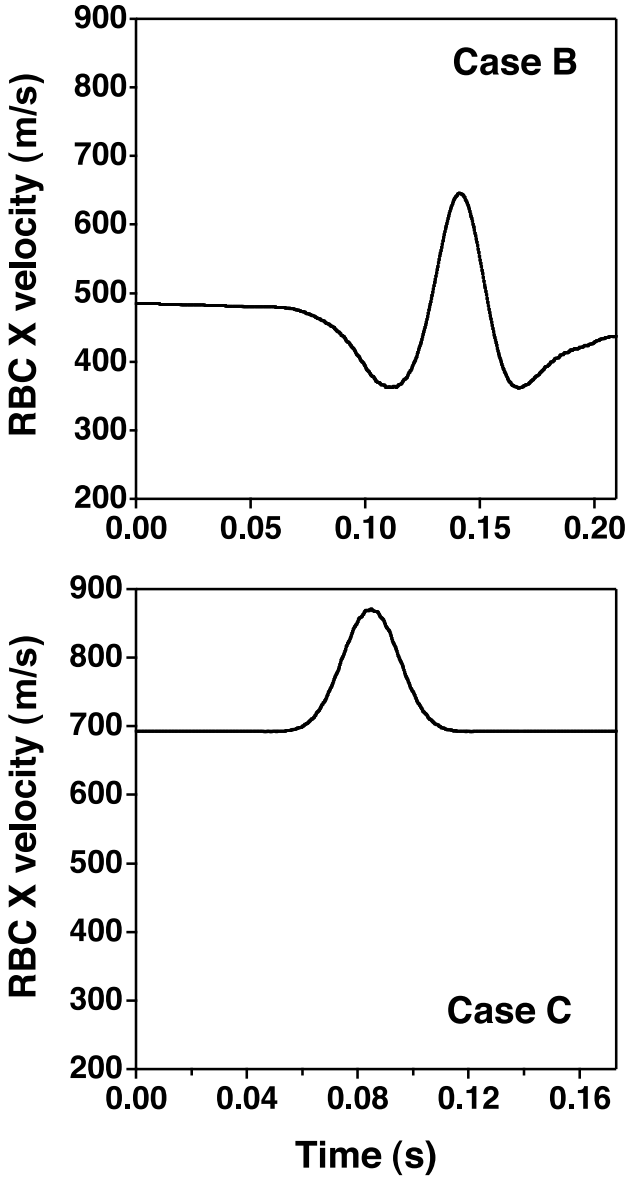

FIGURE 4 Effect of collision height on RBC velocity.

force upon collision is still ~10%, and the behavior is similar to the results of Fig. 3. Remarkably, the normal force profiles mirror those obtained at high shear rate (Fig. 3) with peaks ranging between −10 and +12 pN.

Case C: effect of geometry

One of the most important parameters affecting RBC-leukocyte interaction is the blood hematocrit. RBCs flowing in a tube tend to migrate toward the center of the tube and leave a cell-free layer close to the tube wall (Blackshear et al., 1971; Cokelet and Goldsmith, 1991). This plasma-rich layer is responsible for the Fårhaeus effect, i.e., the increase in discharge hematocrit compared with the tube hematocrit in tubes of diameter less than 150 μm (Skalak and Chien, 1987). At a normal hematocrit the height of the plasma layer can vary between 2 to 6 μm (Blackshear et al., 1971; Cokelet and Goldsmith, 1991). Therefore our case B, where the RBC height is 4.5 μm, represents the interaction between a single RBC and a leukocyte under normal conditions. The purpose of case C is to simulate the forces exerted by RBCs after hemodilution, where the plasma-rich zone is expanded. Therefore, in this case the RBC approaches at a height of 10 μm and undergoes a "glancing" collision with the leukocyte.

The main results of case C are as follows: 1) the RBC is less affected compared with case B. The RBC does not rotate 180° but undergoes a clear oscillation when passing over the leukocyte (Fig. 5 *A*). The precollision velocity of the RBC is 700 μm/s. During interaction it accelerates to 900 followed and then returns to 700 μm/s. This behavior contrasts starkly with that in case B (Fig. 4). 2) The values of the hydrodynamic forces and torques do not change significantly during the glancing RBC-leukocyte collision. However, a small increase in tangential force and torque is recorded (Fig. 5 *B*). The effect of this interaction is much smaller than in case B and the net increase in force/torque and rolling velocity is only ~2%. Notice that the increase is much smaller than in case B, although the relative collision velocity is 40% larger.

DISCUSSION

The presented model predicts a sign reversal on the hydrodynamic normal force, which may help adhesion by deforming the leukocyte and its microvilli, enabling the formation of new bonds. On the other hand, the postcollision detractive hydrodynamic normal force is easily resisted by the existing bonds, requiring only a 3% increase in the overall ligand force. So the net effect of the RBC is to provide an initial normal force to engage additional receptors and ligands as it "bounces" the leukocyte along the endothelium. Just as a small positive force applied to Velcro greatly increases its bond—but a small tug cannot separate it—this bouncing enhances leukocyte adhesion (Munn et al., 1996; Melder et al., 1995, 2000). Noninvasive experiments in flow chambers using a two-photon laser microscopy scanning technique further support these conclusions by showing that the leukocyte distribution across the flow chamber is not affected by the rheological properties of the suspension or the shear rate (data not shown). Therefore, enhancement of leukocyte binding by RBCs (Munn et al., 1996; Melder et al., 2000) cannot be explained by increased leukocyte concentration at the wall, and is probably due to the modulation of the normal force estimated in this work.

We have also shown that the increased tangential force and torque significantly change the rolling velocity of the leukocyte (by 10%). This may initiate rolling in cells previously adherent and therefore may be responsible for the

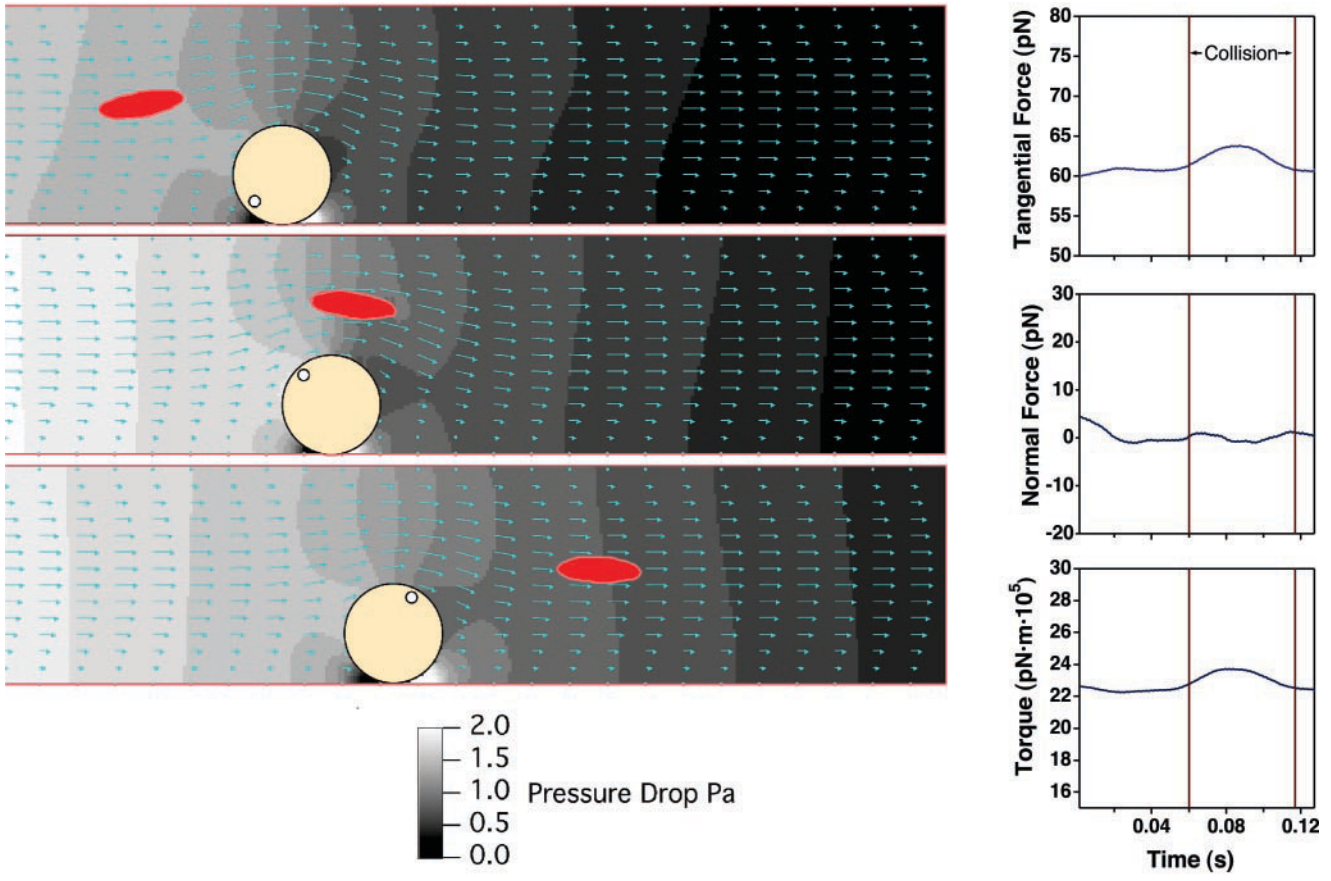

FIGURE 5 Case C simulates a glancing collision between a passing RBC and the rolling leukocyte. (*left*) Flow field at time $t = 0.625, 0.875, 0.119$ s. (*right*) Hydrodynamic tangential force, normal force, and torque profile.

increased rolling fraction of leukocytes seen in experiments (Melder et al., 1995). In additional simulations (not shown), it appears that the confined geometry is responsible for a further increase of 5% to 15% in rolling velocity compared with couette shear flow. These results strongly support the hypothesis that the nature of the contact between the leukocyte and the endothelial wall in vivo (stable adhesion, rolling) and parameters such as rolling velocities cannot be simply extrapolated from RBC-free systems but that the inclusion of the dynamic RBC forces is critical.

Despite the significant effect of the RBC on the local flow field in the small region over the leukocyte, it is remarkable that the hydrodynamic forces are small in case C. This suggests that the height of the collision, and thus the extent of the plasma-rich zone, is a very sensitive parameter even in a small tube. The height of the plasma-rich zone, which depends on hematocrit (Cokelet and Goldsmith, 1991), determines the extent of the leukocyte "envelopment" by the RBCs as seen in case B (Fig. 3 *A*). Our simulation suggests that this envelopment may be the necessary mechanism to exert the required forces. This result is complementary to the experimental observation in model systems that RBCs initiate leukocyte rolling as these cells interact at the entrance to postcapillary venules (Schmid-Schönbein et al., 1980). In fact, the same mechanism simulated in case B—the close "envelopment" of the leukocyte by the RBC—was found to be absolutely necessary to impart the required normal force to initiate leukocyte margination (Schmid-Schönbein et al., 1980).

CONCLUSION

We have, for the first time, modeled the dynamics of leukocyte rolling through the rigorous solution of the unsteady flow field in a confined geometry with and without RBCs. To date, there are several experimental and theoretical studies in the literature reporting forces on adhering cells, but none quantifying forces between rolling leukocytes and flowing RBCs. The forces exerted by a single RBC passing a rolling leukocyte are likely different from those exerted by a concentrated suspension of RBCs and may not be the simple sum of many collisions. In addition, deformable particles may behave differently. Despite its limitations, the current model provides new insight into the essential physics of RBC-leukocyte interactions. Further refinement of

our Lattice Boltzmann algorithms may provide a tool for a direct simulation of a suspension of deformable, interacting particles such as blood in complex and relevant geometries.

The model presented in this work can be applied to other problems that involve interactions mediated by ligands on the surface of the particles or by body forces. For example, leukocyte-leukocyte, leukocyte-platelets, and cell-cell interaction during metastasis and platelet accumulation near the wall could be studied without the shortcomings inherent to other approaches. Further extensions of the model will make it possible to predict the influence of microscopic blood parameters (cell shape, deformability, interaction potential, hematocrit) on commonly-measured bulk properties such as viscosity, thus helping the design of artificial blood substitutes. Other applications such as particle-particle aggregation in emulsion polymerization, coating processes, and aerosol deposition may be envisioned.

We gratefully acknowledge Drs. C. K. Aidun and E.-J. Ding for providing their Lattice Boltzmann codes, upon which this model was constructed, and Dr. N. S. Forbes and B. R. Stoll for helpful discussions. This work was supported by National Institutes of Health Grant R01 HL64240 (to L.L.M.).

REFERENCES

Aidun, C. K., Y. Lu, and E. J. Ding. 1998. Direct analysis of particulate suspensions with inertia using the discrete Boltzmann equation. *J. Fluid Mech.* 373:287–311.

Bernsdorf, J., T. H. Zeiser, G. Brenner, and F. Durst. 1998. Simulation of a 2D channel flow around a square obstacle with lattice-Boltzmann (BGK) automata. *Int. J. Mod. Phys. C.* 9:1192–1141.

Blackshear, P. L., R. J. Forstrom, F. D. Dorman, and G. O. Voss. 1971. Effect of flow on cells near walls. *Fed. Proc.* 30:1600–1611.

Bongrand, P., and G. I. Bell. 1984. Cell-cell adhesion: parameters and possible mechanisms. *In* Cell Surface Dynamics: Concepts and Models. A. Perelson, C. DeLisi, F.W. Wiegel, editors. Marcel Dekker, New York.

Brown, E. B., R. B. Campbell, Y. Tsuzuki, L. Xu, P. Carmeliet, D. Fukumura, and R. K. Jain. 2001. In vivo measurement of gene expression, angiogenesis and physiological function in tumors using multiphoton laser scanning microscopy. *Nat. Med.* 7:864–868.

Chang, K., and D. A. Hammer. 1996. Influence of direction and type of applied force on the detachment of macromolecularly-bound particles from surfaces. *Langmuir.* 12:2271–2282.

Chang, K., D. F. J. Tees, and D. A. Hammer. 2000. The state diagram for cell adhesion under flow: *Proc. Natl. Acad. Sci. U. S. A.* 97: 11262–11267.

Chapman, G. B., and G. R. Cokelet. 1997. Model studies of leukocyte-endothelium-blood interaction. *Biorheology.* 34:37–56.

Chen, H., S. Chen, and W. H. Matthaeus. 1992. Lattice Boltzmann model for simulating flows with multiple phases and components. *Phys. Rev. A.* 45:5339–5342.

Cokelet, G. R., and H. L. Goldsmith. 1991. Decreased hydrodynamic resistance in two-phase flow of blood through small vertical tubes. *Circ. Res.* 68:1–17.

Dong, C., J. Cao, E. J. Struble, and H. H. Lipowsky. 1999. Mechanics of leukocyte deformation and adhesion to endothelium in shear flow. *Ann. Biomed. Eng.* 27:298–312.

Fung, Y. C. 1984. Biodynamics: Circulation. Springer-Verlag, New York.

Goldman, A. J., R. G. Cox, and H. Brenner. 1967. Slow viscous motion of a sphere parallel to a plane wall-II Couette flow. *Chem. Eng. Sci.* 22:653–660.

Graver, D. P., and S. M. Kute. 1998. A theoretical study of the influence of fluid stresses on a cell adhering to a microchannel wall. *Biophys. J.* 75:721–733.

Hammer, D. A., and S. M. Apte. 1992. Simulation of cell rolling and adhesion on surfaces in shear flow: general results and analysis of selectin-mediated neutrophil adhesion. *Biophys. J.* 63:35–57.

Israelachvili, J. N. 1985. Intramolecular and surface forces. Academic Press, New York.

King, M. R., and D. A. Hammer. 2001. Multiparticle adhesive dynamics: interaction between stably and rolling cells. *Biophys. J.* 81:799–813.

Ladd, A. C. J. 1994. Numerical simulations of particulate suspensions via a discretized Boltzmann equation: Part 1. Theoretical foundation. *J. Fluid Mech.* 271:285–309.

Melder, R. J., L. L. Munn, S. Yamada, C. Ohkubo, and R. K. Jain. 1995. Selectin- and integrin mediated T-lymphocyte rolling and arrest on TNF-α-activated endothelium: augmentation by erythrocytes. *Biophys. J.* 69:2131–2138.

Melder, R. J., J. Yuan, L. L. Munn, and R. K. Jain. 2000. Erythrocytes enhance lymphocyte rolling and arrest in vivo. *Microvasc. Res.* 59: 316–322.

Mitchell, D. J., P. Li, P. H. Reinhardt, and P. Kubes. 2000. Importance of L-selectin-dependent leukocyte-leukocyte interaction in human whole blood. *Blood.* 95:2954–2959.

Munn, L. L., R. J. Melder, and R. K. Jain. 1996. Role of erythrocytes in leukocyte-endothelial interactions: mathematical model and experimental validation. *Biophys. J.* 71:466–478.

Phibbs, R. H. 1968. Orientation and distributions of erythrocytes in blood flowing through medium-sized arteries. *In* Hemorheology: Proceedings of the 1st International Conference. A.L. Copley, editor. Pergamon Press, Oxford/New York. pp 617–632.

Qian, Y. H., D. d'Humieres, and P. Lallemand. 1992. Lattice BGK models for Navier-Stokes equations. *Europhys. Lett.* 17:479–483.

Schmid-Schönbein, G. W., Y. C. Fung, and B. Zweifach. 1975. Vascular endothelium-leukocyte interaction: sticking shear force in venules. *Circ. Res.* 39:173–184.

Schmid-Schönbein, G. W., S. Usami, R. Skalak, and S. Chien. 1980. The interaction of leukocytes and erythrocytes in capillary and postcapillary vessels. *Microvasc. Res.* 19:45–70.

Skalak, R., and S. Chien. 1987. Handbook of Bioengineering. McGraw-Hill, New York.

Zao, Y., S. Chien, and S. Weinbaum. 2001. Dynamic contact forces on leukocyte microvilli and their penetration of the endothelial glycocalyx. *Biophys. J.* 80:1124–1140.